

Distributed, communication-efficient, and differentially private estimation of KL divergence

Mary Scott[✉], Sayan Biswas[✉], Graham Cormode[✉], and Carsten Maple[✉]

Abstract

A key task in managing distributed, sensitive data is to measure the extent to which a distribution changes. Understanding this drift can effectively support a variety of federated learning and analytics tasks. However, in many practical settings sharing such information can be undesirable (*e.g.*, for privacy concerns) or infeasible (*e.g.*, for high communication costs). In this work, we describe novel algorithmic approaches for estimating the KL divergence of data across federated models of computation, under differential privacy. We analyze their theoretical properties and present an empirical study of their performance. We explore parameter settings that optimize the accuracy of the algorithm catering to each of the settings; these provide sub-variations that are applicable to real-world tasks, addressing different context- and application-specific trust level requirements. Our experimental results confirm that our private estimators achieve accuracy comparable to a baseline algorithm without differential privacy guarantees.

1 Introduction

Modern applications in data analysis and machine learning work with high-dimensional data to support inferences and provide recommendations [1, 2]. Increasingly, the data to support these tasks comes from individuals who hold their data on personal devices such as smartphones and wearables. In the federated model of computation [3, 4], this data remains on the users’ devices, which collaborate and cooperate to build accurate models by performing computations and aggregations on their locally held information (*e.g.*, training and fine-tuning small-scale models).

A key primitive needed is the ability to compare the distribution of data held by these clients with a reference distribution. For instance, a platform or a service provider would like to know whether the overall behavior of the data is consistent over time for deploying the best fitting and most relevant model. In cases where the data distribution has changed, it may be necessary to trigger model rebuilding or fine-tuning, whereas if there is no change the current model can continue to be used. Hence, we seek ways to measure the similarity of distributions within the federated setting, where strong privacy and security guarantees must be maintained [5, 6], while also ensuring that the computation and communication overheads are bounded.

Among ways to compare probability distributions, the Kullback-Leibler (KL) divergence [7] has been shown to be one of the most accurate and realistic measures in a wide range of contexts including statistics, information theory, and machine learning. Given two distributions P_1 and P_2 defined over the same domain, the KL divergence between them captures the information-theoretic difference of P_1 from P_2 , sometimes expressed as the amount of “surprise” or “information gain” in seeing samples from P_1 when expecting P_2 . If we have a complete representation of P_1 and P_2 to hand, then the KL divergence can be computed directly in its closed form. However, in the federated setting, the test distribution is defined implicitly, based on the empirical frequency of the samples held by a distributed set of clients. In this paper, we develop a *communication-efficient* and *privacy-preserving* method for estimating the KL divergence between distributions under a federated framework.

A trivial solution is for a central server to collect samples from all clients together in a single location, and to evaluate the KL divergence. Although this method gives an accurate answer, it fails to consider privacy or efficiency. Furthermore, the parameter space of the clients’ data can be extremely large, specifically given the availability of clients in modern-day machine learning. Thus, this initial *full-sharing* approach fails to meet the practical requirements of the scenario. The cost overhead will be high: communicating all the samples or their empirical frequencies can consume significant bandwidth, since the number of data points or the domain size can be very large. Moreover, this approach would raise privacy concerns for the participants since it would reveal the samples held by each client directly to the server. Variations on this approach which seek to have clients add noise to the histogram of their item frequencies also fail due to the high domain size involved. Instead, we must seek solutions which reduce the overhead, and provide provable privacy guarantees under various models of trust.

Our approach is to reduce the total communication cost by sampling a subset of clients to participate in building a randomized estimator, and to ensure that differential privacy (DP) is satisfied on the output. Sampling alone is insufficient to solve our problem since it still reveals the sensitive information of the clients included in the sample [8]. For DP, although techniques are known for many problems, the case of KL divergence has not been analyzed previously.

Our contributions are as follows:

- We formalize the problem of federated computation of KL divergence with privacy, and describe three different computational models, based on differing levels of trust.
- We describe a probabilistic estimator for KL divergence based on sampling, and analyze its accuracy. We show how privacy guarantees can be achieved by careful noise addition in each of the three models we consider.
- We present an experimental study of our methods applied to real data, and compare the impact of varying different parameters such as the rate of client sampling and the level of privacy provided.

In what follows, Section 2 describes related work, and we present preliminaries in Section 3. Our main algorithms and their properties are presented in Section 4, while further theoretical analysis is shown in Section 4.2.3. Our experiments are in Section 5, and we make concluding remarks in Section 6.

2 Related Work

The federated model of computation was introduced in its current form by the machine learning community, with a focus on training machine learning (ML) models over distributed data [9]. Since then, work has remained focused on this federated learning (FL) [4], but also broadened to consider a wider range of computational tasks, under the banner of “federated analytics” or “federated computation” [3].

Our focus in this paper is designing randomized algorithms that can operate in the federated setting to estimate the similarity of datasets. This is a task in support of FL, where identifying when a distribution has changed can be important in determining when to improve an existing model via retraining or fine-tuning. Our approach is informed by prior work which has sought to build compact “sketches” for information divergences. We develop a mechanism to privately compare different sets of data across a period of time. It is not possible to assume both distributions are unknown, because the Shift Invariance Theorem [10] means that the distance between them is not estimable in this sketching model. We navigate this issue by instead comparing one publicly known benchmark distribution with a private distribution described by a large group of clients involved in a FL environment.

Our model of privacy adopts DP, a widely-used statistical approach that introduces carefully calibrated randomness into query answers to mask the footprint of any individual in the data [8]. DP has been applied to a wide range of tasks, from gathering basic statistics such as counts and histograms [8] to the optimization of high-dimensional machine learning (ML) models [5]. For distance estimation, results on the privacy properties of the Johnson-Lindenstrauss lemma means that Euclidean distance can be estimated accurately [11,12]. However, apart from this, the study of DP for distance estimation in the federated model has been limited.

There are numerous metrics in the literature for (non-private) distance estimation. The Fréchet distance [13] has been used in the generative adversarial network (GAN) literature to evaluate the distance between real datasets, but it can only be written in closed form if both distributions are Gaussian. The Hölder divergence [14] can only be proper (zero for two identical distributions) given a specific property between conjugate exponents. The Earth-Mover distance [15] produces accurate representations in all spaces except ℓ_1 , causing problems for Laplace distributions. The Kullback-Leibler (KL) divergence [7] is a standard notion of distance that does not have any of the above restrictions. In what follows, we make the KL divergence the focus of our study.

There are a number of ways in which the KL divergence can be approximated. Monte Carlo sampling [16] draws independent and identically distributed (i.i.d.)

samples from the unknown distribution; a good estimator is unbiased and has low variance. Other techniques can be applied when the data is drawn from a parametric distribution, such as Gaussian mixture models [17]. However, we are not aware of any prior work that has studied KL divergence under DP, or in the federated model.

The problem can be approached from a decentralized perspective: this is much more realistic than with a central server because of data sharing laws. To use the aggregate data for learning without compromising on privacy, secure multi-party computation (SMC) can be combined with Gaussian noise scaling to protect all data [18]. Techniques to protect data from malicious clients include zero-knowledge proofs, secret-shared non-interactive proofs [19] and Boolean secret sharing [20]. In the DPrio algorithm [21], clients generate noise then secretly share it with the servers, who then select a small number of clients' noise to add. This improves the data utility of previous methods and ensures DP guarantees and robustness against malicious clients.

3 Preliminaries and Background

3.1 Probability Distributions and Divergences

We consider probability distributions defined empirically by observations of data. Assume that each data point is drawn from a discrete finite domain \mathcal{X} , and write $\mathcal{P}_{\mathcal{X}}$ to be the space of probability distributions on \mathcal{X} . Given a (multi)set of data points of size m , write $D(x)$ for the frequency of x in dataset D . Let P_D be the associated empirical probability distribution, i.e., $P_D(x) = D(x)/m$.

Given two probability distributions P_1 and P_2 , it is natural to want to measure the similarity between them. There are many commonly used statistical divergence measures. For instance, the Total Variation Distance is given by $D_{TV}(P_1, P_2) = \frac{1}{2} \sum_{x \in \mathcal{X}} |P_1(x) - P_2(x)|$. In this paper, our focus will be on the KL divergence between P_1 and P_2 .

Definition 3.1. For discrete probability distributions $P_1, P_2 \in \mathcal{P}_{\mathcal{X}}$, the *Kullback-Leibler (KL) divergence* between P_1 and P_2 , denoted by $D_{\text{KL}}(P_1 \| P_2)$, is defined as:

$$D_{\text{KL}}(P_1 \| P_2) = \sum_{x \in \mathcal{X}} P_1(x) \log \left(\frac{P_1(x)}{P_2(x)} \right).$$

The widespread popularity and many applications of KL divergence make it a first choice for comparing probability distributions.

3.2 Federated Computation

The federated model of computation has recently emerged to capture cases where there are multiple clients holding sensitive data, who wish to co-operate under the guidance of a co-ordinating server to perform a computation over their data [3]. This covers a wide range of scenarios, from cases where there are only

a few powerful clients (*e.g.*, hospitals), to where there are millions or billions of clients (*e.g.*, mobile devices). We will focus on the cases where there is a moderate to large number of relatively weak clients, who are constrained in terms of computation or memory. Within recent research advancements in federated computation, significant attention has focused on federated learning (FL), which aims to build a machine learning model using clients' data. FL can be broadly classified into two categories: *i. horizontal* or *cross-device* FL, where data is partitioned across clients, and all data points held by the clients share the same set of features (*e.g.*, photos stored locally on clients' mobile phones), and *ii. vertical* or *cross-silo* FL, where data is partitioned by features, making it relevant when different entities hold different attributes for the same set of users (*e.g.*, hospitals in the same region specializing in different aspects of healthcare, each holding different pieces of health data for overlapping sets of patients). In typical FL use cases, where clients' data contain sensitive information (*e.g.*, locations, health records, photos, text messages, etc.), it is natural to consider the associated data distribution of the clients as private.

In this paper, we consider a horizontal federated environment consisting of a set of n clients $C = \{c_1, \dots, c_n\}$ for some $n \in \mathbb{N}$ such that all clients independently and honestly comply with the protocol (*i.e.*, there does not exist any Byzantine clients or any adversarial collusion between them). The clients will interact with a co-ordinating server S to compute a function of interest. Let the (private) distribution of the data held across all the clients be $P \in \mathcal{P}_{\mathcal{X}}$, and assume that each client holds data from the set \mathcal{X} .

We identify three variants of the model, split by the level of trust assumed between participants.

- In the *fully trusted federated model (Trusted)*, S is trusted to see true data samples of the clients, but it is desirable to reduce the communication cost compared to centralizing all the data.
- Under the *trusted aggregator model (TAgg)*, a trusted aggregator (TA) receives messages from clients, and reveals only a noisy, aggregated result to the server S .
- For the *fully distributed model (Dist)*, clients make use of distributed noise to ensure that the server S only gets to see the final private estimate without the involvement of any intermediate entity.

These three models trade trust with system complexity and accuracy. We will propose solutions in each of these three models, and contrast their performance theoretically and experimentally.

3.3 Privacy Standards

For privacy, we adopt the textbook DP definition:

Definition 3.2 ((ϵ, δ) -DP [8]). A randomized algorithm \mathcal{M} provides (ϵ, δ) -DP if for any two neighboring datasets D and D' differing in at most one element,

and for any subset of output O , it holds that:

$$\Pr[\mathcal{M}(D) \in O] \leq e^\varepsilon \Pr[\mathcal{M}(D') \in O] + \delta.$$

We will apply the definition to outputs that are histograms. For a finite domain \mathcal{X} , let $\mathcal{H}_{\mathcal{X}} = \{h \mid h: \mathcal{X} \mapsto \mathbb{Z}_{\geq 0}\}$ be the space of all datasets (represented as histograms) whose entries belong to \mathcal{X} , and let $\mathcal{P}_{\mathcal{X}}$ be the space of all probability distributions on \mathcal{X} . Let the *cardinality* of any $h \in \mathcal{H}_{\mathcal{X}}$ be defined as $|h| = \sum_{x \in \mathcal{X}} h(x)$, and let $\psi(h)$ be the empirical distribution on \mathcal{X} that we obtain from h . In other words, $\psi: \mathcal{H}_{\mathcal{X}} \mapsto [0, 1]^{|\mathcal{X}|}$ such that

$$\psi(h) = \{\psi(h)_x: \psi(h)_x = h(x)/|h| \quad \forall x \in \mathcal{X}\}.$$

Definition 3.3 (Adjacent histograms). We call a pair of histograms (*i.e.*, datasets) $h_1, h_2 \in \mathcal{H}_{\mathcal{X}}$ *adjacent*, denoted by $h_1 \sim h_2$, if:

- i. $|h_1|$ and $|h_2|$ are finite
- ii. there are $x_1, x_2 \in \mathcal{X}$, $x_1 \neq x_2$ such that:
 - a. $h_1(x_1) - h_2(x_1) = 1$
 - b. $h_1(x_2) - h_2(x_2) = -1$
 - c. $h_1(x) = h_2(x) \forall x \in \mathcal{X} \setminus \{x_1, x_2\}$.

Definition 3.3 describes dataset pairs that have the same cardinality and differ in the count of exactly one attribute by one. In other words, we call two histograms h_1 and h_2 adjacent if exactly two values they hold are swapped and the count of every other $x \in \mathcal{X}$ is the same in h_1 and h_2 .

Definition 3.4 (Adjacent distributions). We call a pair of distributions $P_1, P_2 \in \mathcal{P}_{\mathcal{X}}$ *adjacent*, denoted by $P_1 \sim P_2$, if there exist $h_1, h_2 \in \mathcal{H}_{\mathcal{X}}$ such that $h_1 \sim h_2$ with $\Pi_1 = \psi(h_1)$ and $\Pi_2 = \psi(h_2)$.

Definition 3.5 (Sensitivity). For any query $f: \mathcal{P}_{\mathcal{X}} \mapsto \mathbb{R}$ on the space of distributions, the *sensitivity of f* is defined as:

$$\Delta(f) = \max_{\substack{P_1, P_2 \in \mathcal{P}_{\mathcal{X}} \\ P_1 \sim P_2}} |f(P_1) - f(P_2)|.$$

A standard technique to obtain DP for a numeric query is to add noise scaled by the sensitivity of the query.

Corollary 3.1 (Gaussian noise [8]). For any $\varepsilon, \delta \geq 0$, it suffices to sample Gaussian noise $\eta_G \sim \mathcal{N}\left(0, \frac{2 \log \frac{1.25}{\delta} \Delta(f)}{\varepsilon}\right)$ and add this to $f(P)$ to provide (ε, δ) -DP for f .

More generally, for any $\mathcal{P}' \subseteq \mathcal{P}(\mathcal{X})$, if $f: \mathcal{P}' \mapsto \mathbb{R}$ is a query on a subspace of $\mathcal{P}_{\mathcal{X}}$, the *sensitivity of f restricted to the subspace \mathcal{P}'* is defined as:

$$\Delta(f|\mathcal{P}') = \max_{\substack{P_1, P_2 \in \mathcal{P}' \\ P_1 \sim P_2}} |\eta(P_1) - \eta(P_2)|.$$

We denote by **SecAgg** a secure aggregation, where the sum of data from multiple sources is computed without revealing any individual inputs. Examples range from a cluster-based model [22] to a privacy-preserving protocol [6] that uses Shamir's t -out-of- n secret sharing scheme [23] to account for dropout clients.

3.4 Monte Carlo subsampling

Recall that the probability distributions P_1 and P_2 are defined via observations of data, therefore we are unable to compute the exact expression of their KL divergence as in Definition 3.1. A common method for constructing an accurate estimate of a sum is to use Monte Carlo subsampling [24]. Given subsamples $x_1, x_2, \dots \sim P_1$, is there an expression that each subsample x_i can be substituted into, such that their sum estimates the KL divergence of P_1 and P_2 ? Using the fact that KL divergence is an example of a Bregman divergence [25], it can be measured as the shortest distance between a convex function and its tangent. Setting $r_i = x_i/P_2$ for subsamples i of P_1 , the estimator $K = (r_i - 1) - \log r_i$ measures the vertical distance between $\log r_i$ and its tangent. K is used as the estimator in Algorithms 1, 2 and 3 in Section 4.

4 Differentially private estimator of KL divergence

4.1 Problem definition

Given a collection of n federated clients whose data collectively defines a data set D , we wish to compute an accurate estimate of the KL divergence between their data distribution and a reference distribution. That is, each client i holds a local dataset D_i , so that $D(x) = \sum_{i=1}^n D_i(x)$. The global dataset D then defines a probability distribution P . The server holds a reference distribution Π , also over \mathcal{X} . For instance, Π could be derived from data collected in the past or in a controlled fashion using voluntary participation of users. The goal is thus to compute $D_{\text{KL}}(\Pi||P)$. We will describe several approaches for the PRIvate ESTimation of KL-Divergence, or PRIEST-KLD for short. We furnish three versions of PRIEST-KLD, namely those which allow us to estimate $D_{\text{KL}}(\Pi||P)$ under the three different levels of trust (Trusted, TAgg or Dist). In the end, the accuracy and privacy guarantees of the estimation of $D_{\text{KL}}(\Pi||P)$ given by PRIEST-KLD, denoted by $D_{\text{KL}}(\Pi||P)_{\text{est}[\lambda, T, \varepsilon, \delta]}^{\text{final}}$, are affected by the *precision parameter* $T \in \mathbb{N}$, the *variance parameter* $\lambda \geq 0$, and the ε and δ parameters for achieving (ε, δ) -DP.

Prior to introducing PRIEST-KLD under the different trust models, we state and prove some useful facts that are necessary to show that the resulting estimators are unbiased.

Fact 4.1. If $\Pi \in \mathcal{P}_{\mathcal{X}}$ is a full-support distribution (i.e., there are no events with zero probability), for any random variable $X \sim \Pi$ and $P \in \mathcal{P}_{\mathcal{X}}$, we have $\mathbb{E} \left[\frac{P(X)}{\Pi(X)} \right] = 1$.

Proof. Letting $r(X) = \frac{P(X)}{\Pi(X)}$:

$$\mathbb{E}_{X \sim \Pi}[r(X)] = \sum_{x \in \mathcal{X}} r(x)\Pi(x) = \sum_{x \in \mathcal{X}} \frac{P(x)}{\Pi(x)}\Pi(x) = \sum_{x \in \mathcal{X}} P(x) = 1.$$

□

Fact 4.2. Under the assumption of Fact 4.1, for any $\lambda > 0$, we have $\mathbb{E} \left[\lambda \left(\frac{P(X)}{\Pi(X)} - 1 \right) - \log \left(\frac{P(X)}{\Pi(X)} \right) \right] = D_{\text{KL}}(\Pi \| P)$.

Proof. Letting $r(X) = \frac{P(X)}{\Pi(X)}$:

$$\begin{aligned} & \mathbb{E}_{X \sim \Pi} [\lambda (r(X) - 1) - \log (r(X))] \\ &= -\mathbb{E}[\log r(X)] \quad (\text{as Fact 4.1} \implies \mathbb{E}[r(X) - 1] = 0) \\ &= -\mathbb{E} \left[\log \frac{P(x)}{\Pi(x)} \right] = \mathbb{E} \left[\log \frac{\Pi(x)}{P(x)} \right] = D_{\text{KL}}(\Pi \| P). \end{aligned}$$

□

In the subsequent analyses of the different trust-based variants of PRIEST-KLD, we shall see that the corresponding estimators have bounded variances and these bounds depend on the choice of the parameter λ . Therefore, it is clearly in our interest to seek a choice of λ that minimizes the variance.

Definition 4.1 (Optimal variance parameter). We call a variance parameter $\lambda_{0,P}$ *optimal* for P under PRIEST-KLD if, for every $\lambda \geq 0$,

$$\text{Var} \left[D_{\text{KL}}(\Pi \| P)_{\text{est}[\lambda_{0,P}, T, \varepsilon, \delta]}^{\text{final}} \right] \leq \text{Var} \left[D_{\text{KL}}(\Pi \| P)_{\text{est}[\lambda, T, \varepsilon, \delta]}^{\text{final}} \right].$$

We omit P from the subscript and refer to the optimal variance parameter as λ_0 if the clients' data distribution P is clear from context.

4.2 PRIEST-KLD: Trusted models

In this section, we focus on models where there is some central entity. For example, this could be a single server or trusted aggregator responsible for carrying out the aggregation of data related to some corresponding FL task, and sharing this data with the main server used for carrying out analytics and publishing the associated results. In particular, in Sections 4.2.1 and 4.2.2 we focus on two different trust models involving a centrally trusted entity: *i.* a federated model with a fully trusted central server and *ii.* a model with a trusted aggregator responsible for collecting the clients' data and sending the result to the server. Section 4.2.3 carries out the theoretical analysis of the privacy guarantees of these two models.

4.2.1 Fully trusted federated model

For the trusted model (Trusted), the server can gather data from clients without any restrictions, and so there is a great deal of flexibility in making an estimate of the KL divergence. A simple approach would be to gather all data from all clients, and use this to compute D_{KL} exactly. However, this is not appropriate for the federated setting, where clients may not always be available to participate, and the communication cost associated with centralizing the data is large. Instead, we propose an approach based on sampling a subset of clients

Algorithm 1: PRIEST-KLD: Trusted federated model

```

1  $S$  samples  $x_t \sim \Pi$  and shares with the clients
2 // Client side:
3 for  $t = 1, \dots, T$  do
4   Set of clients  $C_t \subset C$  sampled to participate in round  $t$ 
5   for  $c \in C_t$  do
6      $c$  reports frequency of  $D_c(x_t)$ 
7      $P(x_t) = \text{SecAgg} \left( \frac{\text{sum}_{c \in C_t} D_c(x_t)}{|C_t|} \right)$ 
8      $r(x_t) = \frac{P(x_t)}{\Pi(x_t)}$  // shared with  $S$ 
9 // Server side:
10  $D_{\text{KL}}(\Pi \| P)_{\text{est}[\lambda, T]}^{\text{prelim}} = \frac{\sum_{t=1}^T \lambda(r(x_t) - 1) - \log r(x_t)}{T}$ 
11  $D_{\text{KL}}(\Pi \| P)_{\text{est}[\lambda_0, T, \varepsilon, \delta]}^{\text{final}} = D_{\text{KL}}(\Pi \| P)_{\text{est}[\lambda_0, T]}^{\text{prelim}} + \eta_{\varepsilon, \delta}$ 
    [where  $\eta_{\varepsilon, \delta}$  is  $(\varepsilon, \delta)$ -DP noise]

```

and securely gathering data from them about their inputs. This sampling-based approach will also inform our subsequent approaches for other models, so we introduce it in some detail here.

Overview of the algorithm. The essence of our approach is to build an estimator for D_{KL} by sampling. The estimator will be a random variable whose expectation and bounded variance will be proven. Finally, we will add noise to the estimator to guarantee DP. This sampling approach leverages a statistical interpretation of D_{KL} : it is the expectation of the log ratio $\log(P_1(\cdot)/P_2(\cdot))$ under the distribution P_1 . Therefore, the server S will sample values from Π , and probe the associated clients for their (empirical) frequencies. This is repeated T times in parallel to reduce the variance. From this, we compute the empirical mean of the observed log ratios. The full algorithm is presented in Algorithm 1.

Analysis of the algorithm. We proceed by studying the expectation and variance of the random variable that captures the algorithm's estimate.

Theorem 4.3. PRIEST-KLD for the Trusted model gives an unbiased estimator of $D_{\text{KL}}(\Pi \| P)$.

Proof.

$$\begin{aligned}
\mathbb{E} \left[D_{\text{KL}}(\Pi \| P)_{\text{est}[\lambda_0, T, \varepsilon, \delta]}^{\text{final}} \right] &= \mathbb{E} \left[D_{\text{KL}}(\Pi \| P)_{\text{est}[\lambda_0, T]}^{\text{prelim}} + \eta_{\varepsilon, \delta} \right] \\
&= \mathbb{E} \left[D_{\text{KL}}(\Pi \| P)_{\text{est}[\lambda_0, T]}^{\text{prelim}} \right] \quad (\text{since } \mathbb{E}[\eta_{\varepsilon, \delta}] = 0) \\
&= \mathbb{E} \left[\frac{1}{T} \left(\sum_{t=1}^T \lambda_0(r(x_t) - 1) - \log r(x_t) \right) \right] \\
&= \frac{T}{T} \mathbb{E}_{X \sim \Pi} [\lambda_0(r(X) - 1) - \log r(X)] \quad (\text{as } x_1, \dots, x_T \sim \Pi) \\
&= D_{\text{KL}}(\Pi \| P) \quad (\text{using Facts 4.1 and 4.2})
\end{aligned}$$

□

The estimator also has a bounded variance.

Theorem 4.4. Under the Trusted model of PRIEST-KLD, if P and Π are full-support distributions, we have

$$\begin{aligned} & \text{Var} \left[D_{\text{KL}}(\Pi \| P)_{\text{est}[\lambda, T, \varepsilon, \delta]}^{\text{final}} \right] \\ & \leq \frac{\lambda^2}{T} (\alpha - 1) + \frac{1}{T} (\max \{ \alpha - 1, \beta^2 - 1 \} + D_{\text{KL}}(\Pi \| P)^2) \\ & \quad - \frac{2\lambda}{T} (D_{\text{KL}}(P \| \Pi) + D_{\text{KL}}(\Pi \| P)) + \sigma_{\varepsilon, \delta}^2, \end{aligned}$$

where $\alpha = \max_{x \in \mathcal{X}} \frac{P(x)}{\Pi(x)}$, $\beta = \max_{x \in \mathcal{X}} \frac{\Pi(x)}{P(x)}$, and $\sigma_{\varepsilon, \delta}^2 = \text{Var} [\eta_{\varepsilon, \delta}]$.

Proof. See Appendix A.1. □

Corollary 4.5. Under the assumptions of Theorem 4.4, we have:

$$0 \leq \lambda_0 \leq \frac{(\alpha\beta - 1)^2}{2\alpha\beta(\alpha - 1)}$$

Proof. From Theorem 4.4, we observe that the upper bound on the variance of our estimator is a convex continuous function of λ . As the optimal λ_0 for our estimator has the least variance under PRIEST-KLD, we consider the upper bound of $\text{Var} \left[D_{\text{KL}}(\Pi \| P)_{\text{est}[\lambda, T, \varepsilon, \delta]}^{\text{final}} \right]$ as a function of λ as derived in Theorem 4.4, compute its derivative with respect to (w.r.t.) λ , and equate it to 0. We obtain:

$$\lambda_0 = \frac{D_{\text{KL}}(P \| \Pi) + D_{\text{KL}}(\Pi \| P)}{\alpha - 1}$$

Using the fact that $D_{\text{KL}}(P \| \Pi) + D_{\text{KL}}(\Pi \| P) \geq 0$ and Dragomir and Gluščević's inequality [26, Theorem 5], we get:

$$\begin{aligned} 0 \leq \lambda_0 & \leq \frac{\frac{(\alpha - \frac{1}{\beta})^2}{4\alpha/\beta} + \frac{(\beta - \frac{1}{\alpha})^2}{4\beta/\alpha}}{\alpha - 1} \\ \implies 0 \leq \lambda_0 & \leq \frac{\frac{\beta}{\alpha} \left(\alpha - \frac{1}{\beta} \right)^2 + \frac{\alpha}{\beta} \left(\beta - \frac{1}{\alpha} \right)^2}{4(\alpha - 1)} = \frac{(\alpha\beta - 1)^2}{2\alpha\beta(\alpha - 1)}. \end{aligned}$$

□

Although we can place a bound on λ_0 , this bound is in terms of α and β (which depend on P), and we would not expect to know these in advance. Consequently, we will seek to find suitable choices of λ that perform well in practice. Note that a suboptimal choice of λ will incur a higher variance for the estimate, but will not affect its unbiasedness (Theorem 4.3).

Algorithm 2: PRIEST-KLD: Trusted aggregator model

```

1  $S$  samples  $x_t \sim \Pi$  and shares with the clients
2 // Client side:
3 for  $t = 1, \dots, T$  do
4   Set of clients  $C_t \subset C$  sampled to participate in round  $t$ 
5   for  $c \in C_t$  do
6      $c$  reports frequency of  $D_c(x_t)$ 
7      $P(x_t) = \text{SecAgg} \left( \frac{\sum_{c \in C_t} D_c(x_t)}{|C_t|} \right)$ 
8      $r(x_t) = \frac{P(x_t)}{\Pi(x_t)}$  // Shared with  $TA$ 
9 // Trusted aggregator side:
10 Share  $A = \sum_{t=1}^T \log(r(x_t)) + \eta'_{\varepsilon, \delta}$  with  $S$ 
11 Share  $B = \sum_{t=1}^T \lambda(r(x_t) - 1) + \eta'_{\varepsilon, \delta}$  with  $S$ 
12 [where  $\eta'_{\varepsilon, \delta}$  is  $(\frac{\sqrt{2}\varepsilon}{T}, \delta)$ -DP noise]
13 // Server side:
14  $D_{\text{KL}}(\Pi \| P)_{\text{est}[\lambda, T, \varepsilon, \delta]}^{\text{final}} = \frac{A+B}{T}$ 

```

4.2.2 PRIEST-KLD: Trusted aggregator (TAgg) model

In the TAgg model, the structure of the estimation algorithm is similar to before, but the tasks are spread out over more participants. The server receives and scales the final output, while the trusted aggregator performs the transformation (logarithm) and aggregation (summation) steps of the results from the participating clients.

Overview of the algorithm. Our approach is similar to the Trusted model, in that noise is still added to the estimator to guarantee DP. However, to reduce our trust in the server S , we introduce a trusted aggregator TA to add noise earlier than the aggregation step, so that S does not view the true values of the clients when it sums their results. The full algorithm is presented in Algorithm 2.

Analysis of the algorithm. We first study the privacy guarantees.

Theorem 4.6. Under the TAgg model, PRIEST-KLD satisfies (ε, δ) -DP.

Proof. Let us denote the non-noisy version of the estimator, *i.e.*, $\frac{\sum_{t=1}^T \lambda(r(x_t) - 1) - \log(r(x_t))}{T}$ by \hat{D} . Let us set $f(P) = D_{\text{KL}}(\Pi \| P)$ for every $P \in \mathcal{P}_{\mathcal{X}}$. The total noise that gets added to \hat{D} to obtain $D_{\text{KL}}(\Pi \| P)_{\text{est}}^{\text{final}}$ is $\frac{2\eta'_{\varepsilon, \delta}}{T}$ where $\eta'_{\varepsilon, \delta} \sim \mathcal{N}\left(0, \frac{2 \log \frac{1.25}{\delta} \Delta(f)}{2\varepsilon/T}\right)$.

This means that $\frac{2\eta'_{\varepsilon, \delta}}{T} \sim \mathcal{N}(0, \sigma^2)$ where

$$\sigma^2 = \frac{4 \log \frac{1.25}{\delta} \Delta(f)}{T \cdot 2\varepsilon/T} = \frac{2 \log \frac{1.25}{\delta} \Delta(f)}{\varepsilon}$$

Thus, $D_{\text{KL}}(\Pi \| P)_{\text{est}[\lambda_0, T, \varepsilon, \delta]}^{\text{final}} = \hat{D} + Z$ where $Z \sim \mathcal{N}\left(0, \frac{2 \log \frac{1.25}{\delta} \Delta(f)}{\varepsilon}\right)$. Using Corollary 3.1, we conclude that $D_{\text{KL}}(\Pi \| P)_{\text{est}[\lambda_0, T, \varepsilon, \delta]}^{\text{final}}$ satisfies (ε, δ) -DP. \square

We now theoretically analyze PRIEST-KLD under the TAgg model to derive an analogous set of results to the Trusted model in Section 4.2.1, using similar lines of argumentation.

Theorem 4.7. PRIEST-KLD under the TAgg model gives an unbiased estimator of $D_{\text{KL}}(\Pi\|P)$.

Proof. By similar arguments to the proof of Theorem 4.6, we observe that $D_{\text{KL}}(\Pi\|P)_{\text{est}[\lambda,T,\varepsilon,\delta]}^{\text{final}} = \hat{D} + Z$ where \hat{D} is an unbiased estimator of $D_{\text{KL}}(\Pi\|P)$ and $Z \sim \mathcal{N}(0, \sigma^2)$. Therefore,

$$\mathbb{E} \left[D_{\text{KL}}(\Pi\|P)_{\text{est}[\lambda,T,\varepsilon,\delta]}^{\text{final}} \right] = \mathbb{E} \left[\hat{D} + Z \right] = \mathbb{E} \left[\hat{D} \right] + \mathbb{E} \left[Z \right] = D_{\text{KL}}(\Pi\|P).$$

□

Theorem 4.8. Under the TAgg model of PRIEST-KLD, if P and Π are full-support distributions, we have

$$\begin{aligned} & \text{Var} \left[D_{\text{KL}}(\Pi\|P)_{\text{est}[\lambda,T,\varepsilon,\delta]}^{\text{final}} \right] \\ & \leq \frac{\lambda^2}{T} (\alpha - 1) + \frac{1}{T} (\max \{ \alpha - 1, \beta^2 - 1 \} + D_{\text{KL}}(\Pi\|P)^2) \\ & \quad - \frac{2\lambda}{T} (D_{\text{KL}}(P\|\Pi) + D_{\text{KL}}(\Pi\|P)) + \sigma_{\varepsilon,\delta}^2, \end{aligned}$$

where α, β and σ are the same as in Theorem 4.4.

Proof.

$$\begin{aligned} & \text{Var} \left[D_{\text{KL}}(\Pi\|P)_{\text{est}[\lambda,T,\varepsilon,\delta]}^{\text{final}} \right] \\ & = \text{Var} \left[\frac{\sum_{t=1}^T \lambda(r(x_t) - 1) - \log(r(x_t))}{T} \right] + \text{Var} \left[\frac{2\eta'_{\varepsilon,\delta}}{T} \right] \\ & \leq \frac{\lambda^2}{T} (\alpha - 1) + \frac{1}{T} (\max \{ \alpha - 1, \beta^2 - 1 \} + D_{\text{KL}}(\Pi\|P)^2) \\ & \quad - \frac{2\lambda}{T} (D_{\text{KL}}(P\|\Pi) + D_{\text{KL}}(\Pi\|P)) + \frac{4\sigma_{\varepsilon,\delta}'^2}{T^2} \\ & \quad \left(\text{where } \sigma_{\varepsilon,\delta}'^2 = \text{Var} [\eta'_{\varepsilon,\delta}] \right) \\ & \leq \frac{\lambda^2}{T} (\alpha - 1) + \frac{1}{T} (\max \{ \alpha - 1, \beta^2 - 1 \} + D_{\text{KL}}(\Pi\|P)^2) \\ & \quad - \frac{2\lambda}{T} (D_{\text{KL}}(P\|\Pi) + D_{\text{KL}}(\Pi\|P)) + \sigma_{\varepsilon,\delta}^2, \end{aligned}$$

noting that $\frac{4\sigma_{\varepsilon,\delta}'^2}{T^2} = \sigma_{\varepsilon,\delta}^2$ and using similar reasoning as in the proof of Theorem 4.4. □

Remark 1. Since, by Theorem 4.8, the upper bounds for the variance of our estimator in the TAgg and Trusted models are the same, it is straightforward to derive that the corresponding λ_0 under the TAgg model will also have the same bounds, *i.e.*, $0 \leq \lambda_0 \leq \frac{(\alpha\beta-1)^2}{2\alpha\beta(\alpha-1)}$.

4.2.3 Privacy analysis

Although the details of adding noise for privacy guarantees differ across the two models discussed above, the analysis of the output and the corresponding sensitivity analysis (essential for satisfying DP) are identical across the two settings¹. Therefore, in this section, we carry out the privacy analysis catering to both TAgg and Trusted.

For any $P \in \mathcal{P}_{\mathcal{X}}$ representing the data distribution of participating clients and $\Pi \in \mathcal{P}_{\mathcal{X}}$ serving as the reference (non-private) distribution to be compared with P , we fix $\eta(P) = D_{\text{KL}}(\Pi \| P)$ as the true KL divergence between Π and P , and $\hat{\eta}(P) = D_{\text{KL}}(\Pi \| P)_{\text{est}[\lambda_0, P, T, \varepsilon, \delta]}^{\text{final}}$ as the estimate of the KL divergence between Π and P as given by PRIEST-KLD. We now analyze the impact of the DP noise we have introduced on the sensitivity of η and $\hat{\eta}$.

Let $\mathcal{H}_{\mathcal{X}}^{>1} = \{h \in \mathcal{H}_{\mathcal{X}} : h(x) > 1 \forall x \in \mathcal{X}\}$ be the space of all datasets where each value from \mathcal{X} occurs at least twice. Similarly, let $\mathcal{P}^{>1} \subset \mathcal{P}_{\mathcal{X}}$ be corresponding probability distributions such that

$$\mathcal{P}^{>1} = \{\Pi \in \mathcal{P}_{\mathcal{X}} : \psi^{-1}(\Pi) \in \mathcal{H}_{\mathcal{X}}^{>1}\}.$$

Theorem 4.9. For $\mathcal{H}_{\mathcal{X}}^{>1}$ with a fixed cardinality, $\Delta(\eta | \mathcal{P}^{>1}) < 0.7$.

Proof. For distributions $P_1, P_2 \in \mathcal{P}^{>1}$ such that $P_1 \sim P_2$, there must be histograms $h_1, h_2 \in \mathcal{H}_{\mathcal{X}}^{>1}$ with $h_1 \sim h_2$ satisfying $P_1 = \psi(h_1)$ and $P_2 = \psi(h_2)$. Thus, there must be some $x_1, x_2 \in \mathcal{X}$ such that $h_1(x_1) - h_2(x_1) = 1$, $h_1(x_2) - h_2(x_2) = -1$ and $h_1(x) = h_2(x) \forall x \in \mathcal{X} \setminus \{x_1, x_2\}$. Let $N = |h_1| = |h_2|$, $n_1 = h_1(x_1)$, and $n_2 = h_1(x_2)$. Because $h_1(x) = h_2(x)$ for $x \in \mathcal{X} \setminus \{x_1, x_2\}$, let the value of $h_1(x_1) + h_1(x_2) = h_2(x_1) + h_2(x_2)$ be denoted by k . Note that $P_1, P_2 \in \mathcal{P}^{>1}$ implies that $k \geq 4$ (because each value from \mathcal{X} occurs at least twice). Therefore,

$$\begin{aligned} |\eta(P_1) - \eta(P_2)| &= \left| \sum_x \Pi(x) \log \frac{\Pi(x)}{P_1(x)} - \sum_x \Pi(x) \log \frac{\Pi(x)}{P_2(x)} \right| \\ &= \left| \sum_x \Pi(x) \log \frac{P_2(x)}{P_1(x)} \right| \\ &= \left| \Pi(x_1) \log \frac{h_2(x_1)}{h_1(x_1)} + \Pi(x_2) \log \frac{h_2(x_2)}{h_1(x_2)} \right| \\ &= \left| \Pi(x_1) \log \frac{n_1}{n_1 - 1} + \Pi(x_2) \log \frac{n_2 + 1}{n_2} \right| \\ &= \left| \Pi(x_1) \log \left(1 - \frac{1}{n_1} \right) + \Pi(x_2) \log \left(1 + \frac{1}{k - n_1} \right) \right| \\ &\leq \left| \Pi(x_1) \log \left(1 - \frac{1}{n_1} \right) \right| + \left| \Pi(x_2) \log \left(1 + \frac{1}{k - n_1} \right) \right| \\ &= \Pi(x_1) \log \left(1 + \frac{1}{n_1 - 1} \right) + \Pi(x_2) \log \left(1 + \frac{1}{k - n_1} \right) \end{aligned}$$

¹TAgg essentially “splits” the noise in two different segments to foster the same DP guarantee as Trusted.

$$\begin{aligned}
&\leq \Pi(x_1) \log \left(1 + \frac{1}{n_1 - 1} \right) + \Pi(x_2) \log \left(1 + \frac{1}{(n_1 + 2) - n_1} \right) \\
&\text{[as } k \geq n_1 + 2 \text{ and } \Pi(x_2) \log \left(1 + \frac{1}{k - n_1} \right) \text{ decreases with } k\text{]} \\
&\leq \Pi(x_1) \log \left(1 + \frac{1}{n_1 - 1} \right) + \Pi(x_2) \log \frac{3}{2} \\
&\leq \Pi(x_1) \log \left(1 + \frac{1}{2 - 1} \right) + \Pi(x_2) \log \frac{3}{2} \\
&\text{[as } n_1 \geq 2 \text{ and } \Pi(x_1) \log \left(1 + \frac{1}{n_1 - 1} \right) \text{ decreases with } n_1\text{]} \\
&\leq \log 2 \cdot (\Pi(x_1) + \Pi(x_2)) \leq \log 2 < 0.7.
\end{aligned}$$

□

Theorem 4.10. For $\mathcal{H}_{\mathcal{X}}^{>1}$ with a fixed cardinality,

$$\Delta(\hat{\eta} | \mathcal{P}^{>1}) \leq (\hat{\alpha} - 1) |\lambda_{0,P_1} - \lambda_{0,P_2}| + \frac{\lambda_{0,P_2}}{Nm} + \log 2,$$

where

$$\hat{\alpha} = \max \left\{ \max_{x \in \mathcal{X}} \frac{P_1(x)}{\Pi(x)}, \max_{x \in \mathcal{X}} \frac{P_2(x)}{\Pi(x)} \right\} \text{ and } m = \min_{x \in \mathcal{X}} \Pi(x).$$

Proof. See Appendix A.2. □

4.3 PRIEST-KLD: Fully distributed model

In the distributed (Dist) model, the clients are responsible for adding local noise to their samples before they are released to the server. As the server does not see any data in the clear, it does not have to be trusted. Moreover, there is no requirement for an intermediate entity acting as a trusted aggregator in this model. The noise each client must add to their data to ensure DP can be computed via its local model [8].

Overview of the algorithm. This approach is different to the Trusted and TAgg models, in that noise is added by the clients to guarantee DP. The small constant $\tau > 0$ is required to ensure that $r'(x_t) > 0$ and, therefore, its logarithm is well-defined. The full algorithm is presented in Algorithm 3.

Analysis of the algorithm. The privacy properties of Algorithm 3 follow directly from the noise addition to the (aggregated) input.

Theorem 4.11. PRIEST-KLD under the Dist model guarantees (ε, δ) -DP.

Proof. If we consider example-level DP, then making one change to the input can change $P(x_t)$ by at most $1/N$, where N is the number of samples x_t . Moreover, looking at $P(x_t)$ for a collection of samples x_t can be considered as a histogram query, so we can add total noise with sensitivity $2/N$ to each sampled item. Consequently, we obtain an (ε, δ) -DP guarantee by adding the noise as specified in Algorithm 3. □

Algorithm 3: PRIEST-KLD: Fully distributed model

```
1  $S$  samples  $x_t \sim \Pi$  and shares with the clients
2 // Client side:
3 for  $t = 1, \dots, T$  do
4     Set of clients  $C_t \subset C$  sampled to participate in round  $t$ 
5     for  $c \in C_t$  do
6          $c$  reports frequency of  $D_c(x_t)$ 
7          $P(x_t) = \text{SecAgg} \left( \frac{\sum_{c \in C_t} D_c(x_t)}{|C_t|} \right)$ 
8          $P'(x_t) = \max\{P(x_t) + \eta_{\varepsilon, \delta}, \tau\}$  // Shared with  $S$ 
9         [ $\eta_{\varepsilon, \delta}$  is  $\left(\frac{\sqrt{2\varepsilon}}{N}, \delta\right)$ -DP noise,  $N$  is # samples  $x_t$  and  $\tau > 0$  is small
            constant]
10         $r(x_t) = \frac{P'(x_t)}{\Pi(x_t)}$ 
11 // Server side:
12  $D_{\text{KL}}(\Pi \| P)_{\text{est}[\lambda, T]}^{\text{prelim}} = \frac{\sum_{t=1}^T \lambda(r'(x_t) - 1) - \log r'(x_t)}{T}$ 
13  $D_{\text{KL}}(\Pi \| P)_{\text{est}[\lambda_0, T, \varepsilon, \delta]}^{\text{final}} = D_{\text{KL}}(\Pi \| P)_{\text{est}[\lambda_0, T]}^{\text{prelim}}$ 
```

However, note that PRIEST-KLD for the Dist model does not give an unbiased estimator of $D_{\text{KL}}(\Pi \| P)$, due to the correction factor of τ to avoid negative values of the estimated ratio $r(x_t)$. Therefore, a proof such as Theorem 4.3 or Theorem 4.7 would not be applicable. Instead, we will rely on the empirical evaluation to compare the suitability of the Dist approach for federated KL divergence estimation.

5 Experimental evaluation

We implemented the Trusted, TAgg and Dist models of PRIEST-KLD, displayed in Algorithms 1, 2 and 3 respectively, in Python to evaluate their performance. We performed evaluation on the FEMNIST dataset, a benchmark from the FL community [27]. The data is a collection of images of handwritten digits 0-9, where the image data is partitioned based on the writer of the digit. In all experiments, a set of clients C_t is chosen in round t independent of the past rounds. Their images are then added to 10 separate stores, each containing images labeled as one of the digits 0-9. To generate a meaningful distribution for each of these stores, each 28×28 image is partitioned into sixteen 7×7 sub-images, with the mean intensity of each sub-image computed and mapped to a binary level, and the probabilities of encountering each of the $2^{16} = 65536$ possibilities listed. Note that in practice, for a 1400-image sample, a subset of these possibilities would typically occur. Thereafter, it is simple to use these probabilities to compute the KL divergence between the estimated distributions of any non-identical pair of digits. Concerning these pairs, the evaluations will relate to the statistics associated with:

- the *mean* measured across all 90 distinct pairs,
- the pair with the *lowest* KL divergence (min pair),
- and the pair with the *highest* KL divergence (max pair).

5.1 Choices of lambda

The performance of each of the PRIEST-KLD models is evaluated using the *mean squared error (MSE)*, defined as the squared difference between the estimator in question and the ground truth. Contrasting privacy levels $\varepsilon \in [0.05, 6]$ and client sample sizes $|C_t| \in [36, 660]$ are explored. The range of ε and the constant $\delta = 0.05$ are chosen such that common settings from the privacy literature are represented [8, 28–31]. The benefit of providing a level of privacy beyond the upper limit $\varepsilon = 6$ declines significantly. The percentage of clients chosen in each round ranges from approximately 1% to 20% of the total number available, mirroring the proportion sampled in similar studies [9, 32, 34]. Whether the mean MSE is computed across all 90 distinct pairs, or for the pair with the lowest or highest KL divergence, we seek the $\lambda \in [0, 2]$ that minimizes the MSE. In Section 5.2, each of these best values of λ is fixed in the three models of PRIEST-KLD, and their resulting accuracy analyzed.

5.1.1 Privacy levels

Three values $\varepsilon = 0.05, 0.5$ and 3 are each tested, with $|C_t| = 200$ (approximately 5% of clients) also fixed.

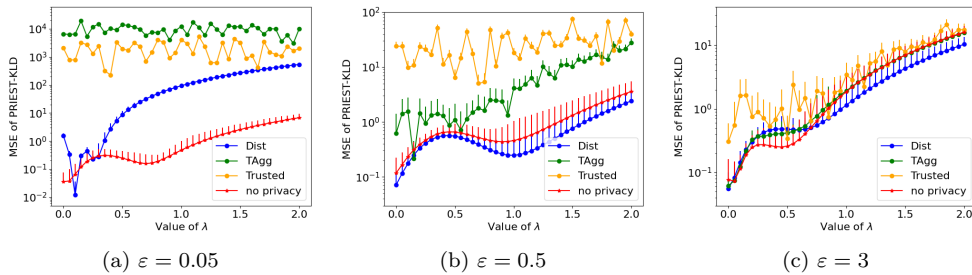


Figure 1: Effect of λ on mean MSE of PRIEST-KLD models, fixing $|C_t| = 200$.

Figure 1(a) confirms that when ε is small (high privacy), Dist produces the lowest mean MSE, and deviates the least from the baseline model. The effect of λ on the mean MSE of Dist is expected: its general increase is due to the linear relationship between λ and D_{KL} , and the fluctuations at low values of λ can be explained by the numerator of D_{KL} changing sign. In particular, the best value of λ in this case is 0.1. Note that the mean MSE of Trusted and TAgg fluctuate at around 10^3 and 10^4 respectively without a clear dependence on λ , so it does not make sense to discuss their best λ . This is explained by the small ε creating a level of noise several orders of magnitude larger than in Dist or the baseline model, accounting for most of the mean MSE and causing λ to not have an impact. Figures 1(b) confirms that when ε is moderate (moderate privacy), Dist

still produces the lowest mean MSE even though, as expected, the mean MSE of all three models have decreased by several orders of magnitude. Note that the decrease in noise seems to have affected the TAgg model the most, especially with its MSE now increasing with λ . This is because the level of trust in TAgg is lower than Trusted and higher than Dist, and with the noise of Dist already low at high privacy, it can decrease more in the TAgg model. The mean MSE of the Trusted model is still fluctuating because the level of noise required for DP is still too high for λ to have an impact. The linear relationship between λ and D_{KL} for all models ensures that when λ has an impact, the mean MSE of the relevant model increases with λ . This is apparent in Figure 1(b) and (c), with $\lambda = 0$ being the best choice for these models. When ε is high (low privacy), all models have a similar mean MSE, signifying the minimal impact of noise. To encompass all models and values of ε , we can choose a recommended value of $\lambda = 0.1$. For the pairs with the lowest and highest KL divergence respectively, a similar analysis results in choices $\lambda = 0.25$ and $\lambda = 0.05$ respectively.

5.1.2 Client sample sizes

Three contrasting values $|C_t| = 36, 270$ and 540 (approximately 1%, 7% and 14% of clients, respectively) are considered, with $\varepsilon = 0.5$ also fixed.

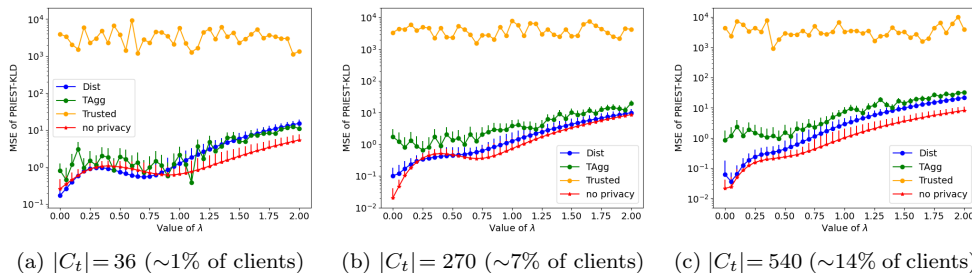


Figure 2: Effect of λ on mean MSE of PRIEST-KLD models, fixing $\varepsilon = 0.5$.

In all subfigures of Figure 2, it is apparent that the Dist and TAgg models are favored over the Trusted model. Not only do the former have a significantly lower mean MSE than the latter, but they have a clear dependence on λ that makes it easier to pick the best value. As we have seen in the trends with $\varepsilon = 0.5$, the Trusted model requires a level of noise that is much larger than the impact of λ . In Figure 2(a), when approximately 1% of clients are sampled ($|C_t| = 36$), both Dist and TAgg closely follow the trend of the baseline model with no privacy, with best values $\lambda = 0$ and $\lambda = 1.1$ respectively. In Figure 2(b) and (c), when approximately 7% ($|C_t| = 270$) and 14% ($|C_t| = 540$) of clients are sampled respectively, Dist has a lower mean MSE than TAgg for all values of λ , with the former following the trend of the baseline model more closely than the latter. This upward trend in the mean MSE of Dist and TAgg with λ was already explained in their relationship with changing ε . Dist and TAgg have best values $\lambda = 0$ and $\lambda = 0.25$ respectively when $|C_t| = 270$, and $\lambda = 0.05$ and $\lambda = 0$ respectively when $|C_t| = 540$. Note that, as $|C_t|$ increases, the mean MSE of Dist and TAgg decreases. This is expected because having larger samples of

clients provides a more accurate estimate of the output of PRIEST-KLD. To minimize the mean MSE of all models in all four subfigures, a best value $\lambda = 0.05$ is selected. For the pairs with the lowest and highest KL divergence respectively, a similar analysis results in choices $\lambda = 0.15$ and $\lambda = 0$ respectively.

5.2 Performance of PRIEST-KLD models

For both low and high KL divergence, the best $\lambda \in [0, 2]$ is chosen in order to reduce the MSE according to the values seen in the previous section. The setting of ε will also affect the noise-to-estimate ratio, and our experiments will plot the impact of this as ε ranges from small (high privacy) to large (weaker privacy).

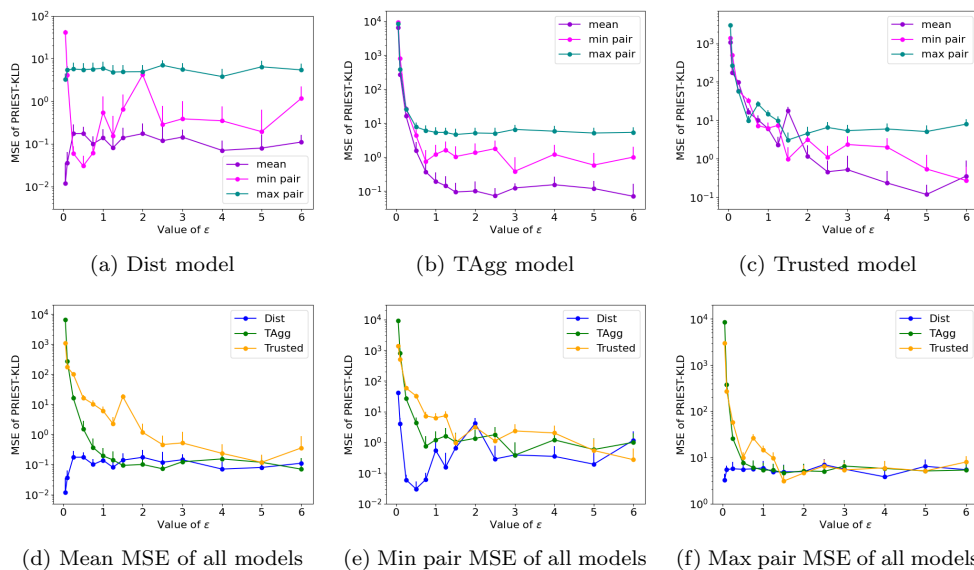


Figure 3: Effect of ε on MSE of PRIEST-KLD models, fixing $|C_t| = 200$.

5.2.1 Privacy levels

Here, the privacy parameter $\varepsilon \in [0.05, 6]$ is varied and the client sample size $|C_t| = 200$ is fixed.

The MSE of Dist in Figure 3(a) is low and fluctuating regardless of the value of ε , while the MSE of TAgg in Figure 3(b) and Trusted in Figure 3(c) is significantly larger when ε is close to 0, decreasing exponentially as ε increases to 3. Though we would expect the MSE of Dist to drop as ε increases, the fact that the optimum λ is such an outlier for low ε in Figure 1(a) ensures that its MSE is brought down to the same level as the larger values of ε . The same trends are present whether the mean MSE across all pairs is computed, or the MSE of the pair with the lowest or highest KL divergence. The fact that the MSE of the min pair is much closer to the mean MSE than the MSE of the max pair, regardless of the model, indicates that most of the pairs have low KL divergence. Figures 3(d), (e) and (f) compare the MSE of all PRIEST-KLD models and confirm that for low ε (high privacy regime), Dist is heavily favored over TAgg

and Trusted. It can be noted that $\varepsilon = 0.5$ produces a low MSE for all models while providing a good level of formal privacy guarantee.

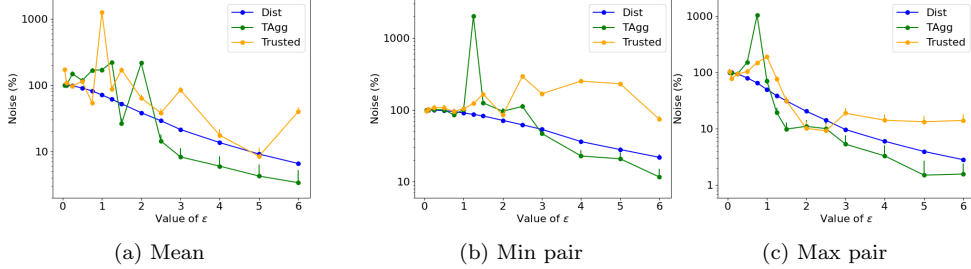


Figure 4: Effect of ε on percentage of D_{KL} that is noise, fixing $|C_t|=200$.

Figures 4(a) and 4(b) display the proportion of noise for the mean of all 90 distinct pairs, as well as the pair with the lowest and highest KL divergence (min pair and max pair) respectively. This proportion is computed by dividing the total noise requirement of a model by its ground truth. For all models of PRIEST-KLD in both graphs, with the exception of Trusted in Figure 4(b), the proportion of noise decreases exponentially as the value of ε increases. This is consistent with Corollary 3.1, which confirms that the noise required has a logarithmic relationship with the reciprocal of ε (i.e., an exponential relationship with ε). Dist requires a lower proportion of noise than TAgg for smaller values of ε , with the opposite true for larger values of ε . Both Dist and TAgg require a lower proportion of noise than Trusted in general. This is consistent with the literature, as a higher noise level implies a stronger privacy guarantee [33, 34].

5.2.2 Client sample sizes

Here, the size of selected clients $|C_t| \in [36, 660]$ is varied and the privacy parameter ε is initially set to 0.5.

It is apparent from Figure 5(a) that with this value of ε , the mean MSE of all models does not have a clear dependence on the client sample size $|C_t|$. Recall from Algorithms 1, 2 and 3 that the more clients there are, the more accurate the estimation should be. A reasonable hypothesis is that $\varepsilon = 0.5$ is too low to display the dependence of the mean MSE on $|C_t|$, producing a high level of noise that obscures this trend. Instead, we fix $\varepsilon = 2$ and $\varepsilon = 5$ in turn, displaying the trends in Figures 5(b) and (c) respectively. In both graphs, it is now clear for TAgg and Dist that as the client sample size increases, the accuracy of the estimator improves more closely to the baseline model than for $\varepsilon = 0.5$. Note that $|C_t|=360$ produces a mean MSE significantly lower than smaller sample sizes, and almost as low as $|C_t|=660$. This value of $|C_t|$ corresponds to sampling approximately 10% of clients per round. Though the accuracy of Trusted is not affected by the client sample size, it does improve significantly as ε increases, reflecting the decrease in noise that we hypothesized. Note that increasing ε from 2 to 5 does not improve the accuracy of the estimator, while the decrease in the level of noise leaves the data more at risk of being compromised. Therefore, $\varepsilon = 2$ produces a good trade-off between displaying the trends of Algorithms 1, 2 and

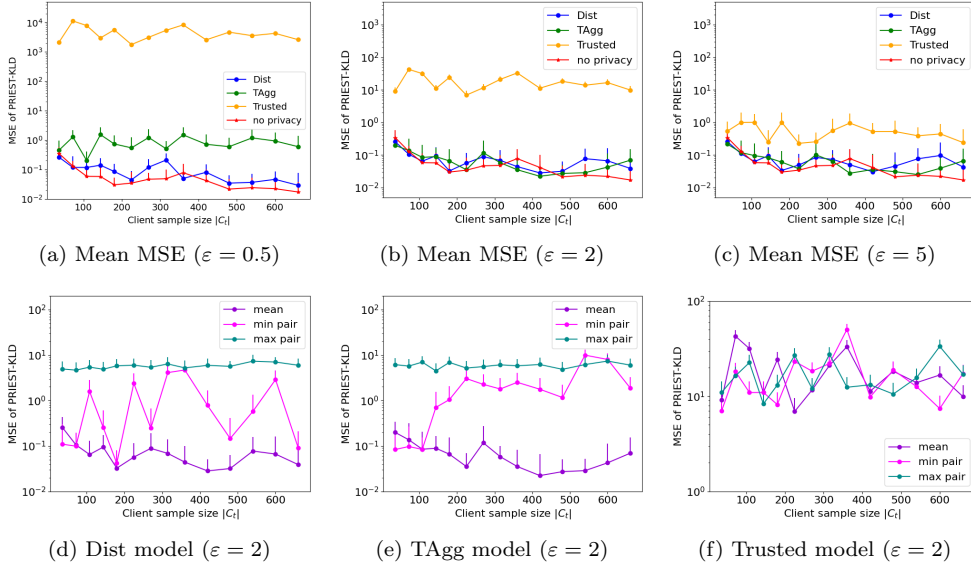


Figure 5: Effect of $|C_t|$ on MSE of PRIEST-KLD models, fixing $\epsilon = 0.5$, $\epsilon = 2$ or $\epsilon = 5$.

3 ensuring strong DP guarantees, with TAgg and Dist favored over Trusted. For the remaining graphs, we fix $\epsilon = 2$.

Figures 5(d), (e) and (f) add the MSE of the min pair and max pair to the mean MSE of each model. The additional lines are not expected to have the same dependence on $|C_t|$, because the identity of the min pair and max pair change every round by definition. The purpose of these graphs, however, are to emphasize the dependence of the mean MSE on $|C_t|$ when TAgg and Dist are used, and to show that the mean MSE is favored over that of the min pair and max pair for most values of $|C_t|$.

5.3 Evaluation

In this experimental study, we have explored the performance of all models of PRIEST-KLD, the settings and trends of the parameter λ that ensure these models perform at their best, and how their utility is affected by the parameter ϵ . It is clear that in general the Dist model gives a more accurate result than the TAgg and Trusted models, and the more substantial analyses related to the former model succeed in filling the gaps present in its theoretical analysis in Section 4.3.

In Section 5.1 we studied how to select the values of λ that resulted in the best accuracy of the models of PRIEST-KLD at contrasting privacy levels and client sample sizes. For real-world applications that require a particular level of privacy or client sample size, these values of λ can be substituted into Algorithms 1, 2 or 3 to ensure that the relevant model can perform at its best.

In Section 5.2 it was established that all models of PRIEST-KLD have better accuracy when ϵ is large. A sufficiently large value of ϵ also ensures that the level of noise does not obstruct the dependence on the client sample size.

However, as the level of privacy is an important factor, it is better to choose the smallest acceptable ε to get the best privacy-accuracy trade-off. Using a similar method, it was established that sampling approximately 10% of clients per round produces a good trade-off between the accuracy of PRIEST-KLD and its computational complexity. The Dist and TAgg models are favored over the Trusted model, and the mean MSE is favored over that of the min pair and max pair.

6 Concluding Remarks

In this paper, we have proposed PRIEST-KLD, a novel class of randomized algorithms that can privately estimate the similarity of datasets in the federated setting with a significant improvement in communication efficiency. We combine the theory of DP, FL, secure aggregation and Monte Carlo subsampling for PRIEST-KLD to cater to three contrasting trust models that trade-off trust with system complexity and accuracy. We confirm empirically that our estimator for each model has the desired properties, and find parameter settings that ensure a high level of accuracy while simultaneously preserving privacy. Future directions include formulating an unbiased fully distributed model in such a way that the complexity of theoretical expressions is not a limiting factor, and studying the experimental trends of the trusted models in more detail.

A Postponed Proofs

A.1 Proof of Theorem 4.4

$$\begin{aligned}
& \text{Var} \left[D_{\text{KL}} (\Pi \| P)_{\text{est}[\lambda_0, T, \varepsilon, \delta]}^{\text{final}} \right] = \text{Var} \left[D_{\text{KL}} (\Pi \| P)_{\text{est}[\lambda_0, T]}^{\text{prelim}} + \eta_{\varepsilon, \delta} \right] \\
& = \text{Var} \left[\frac{\sum_{t=1}^T \lambda_0 (r(x_t) - 1) - \log r(x_t)}{T} \right] + \sigma_{\varepsilon, \delta}^2 \\
& = \frac{1}{T^2} \sum_{t=1}^T (\lambda_0^2 \text{Var}[r(x_t) - 1] + \text{Var}[\log r(x_t)]) \\
& \quad - 2\lambda_0 (\text{Cov} [(r(x_t) - 1), \log r(x_t)]) + \sigma_{\varepsilon, \delta}^2 \\
& = \sigma_{\varepsilon, \delta}^2 + \frac{1}{T^2} \sum_{t=1}^T (\lambda_0^2 \text{Var}[r(x_t)] + \text{Var}[\log r(x_t)]) \\
& \quad - 2\lambda_0 (\mathbb{E} [(r(x_t) - 1) \log r(x_t)] - \mathbb{E}[r(x_t) - 1] \mathbb{E}[\log r(x_t)]) \\
& = \sigma_{\varepsilon, \delta}^2 + \frac{1}{T^2} \sum_{t=1}^T (\lambda_0^2 \text{Var}[r(x_t)] + \text{Var}[\log r(x_t)]) \\
& \quad - 2\lambda_0 (\mathbb{E}[r(x_t) \log r(x_t)] - \log r(x_t)) \\
& [\cdot \text{ Fact 4.1} \implies \mathbb{E}[r(x_t) - 1] = 0]
\end{aligned}$$

$$\begin{aligned}
&= \sigma_{\varepsilon, \delta}^2 + \frac{1}{T^2} \sum_{t=1}^T (\lambda_0^2 \text{Var}[r(x_t)] + \text{Var}[\log r(x_t)]) \\
&\quad - 2\lambda_0 \mathbb{E}[r(x_t) \log r(x_t)] + 2\lambda_0 \mathbb{E}[\log r(x_t)] \\
&= \sigma_{\varepsilon, \delta}^2 + \frac{1}{T^2} \sum_{t=1}^T (\lambda_0^2 \text{Var}[r(x_t)] + \text{Var}[\log r(x_t)]) \\
&\quad - \frac{2\lambda_0 T}{T^2} \sum_{x \in \mathcal{X}} \frac{P(x)}{\Pi(x)} \log \frac{P(x)}{\Pi(x)} \Pi(x) + \frac{2\lambda_0 T}{T^2} \sum_{x \in \mathcal{X}} \log \frac{P(x)}{\Pi(x)} \Pi(x) \\
&= \sigma_{\varepsilon, \delta}^2 + \frac{1}{T^2} \sum_{t=1}^T (\lambda_0^2 \text{Var}[r(x_t)] + \text{Var}[\log r(x_t)]) \\
&\quad - \frac{2\lambda_0}{T} (D_{\text{KL}}(P \parallel \Pi) + D_{\text{KL}}(\Pi \parallel P)) \\
&= \sigma_{\varepsilon, \delta}^2 + \frac{1}{T^2} \sum_{t=1}^T (\lambda_0^2 \text{Var}[r(x_t)] + \mathbb{E}[\log^2 r(x_t)] - \mathbb{E}^2[\log r(x_t)]) \\
&\quad - \frac{2\lambda_0}{T} (D_{\text{KL}}(P \parallel \Pi) + D_{\text{KL}}(\Pi \parallel P)) \\
&= \sigma_{\varepsilon, \delta}^2 + \frac{1}{T^2} \sum_{t=1}^T (\lambda_0^2 \text{Var}[r(x_t)] + \mathbb{E}[\log^2 r(x_t)]) \\
&\quad + \frac{T}{T^2} D_{\text{KL}}(\Pi \parallel P)^2 - \frac{2\lambda_0}{T} (D_{\text{KL}}(P \parallel \Pi) + D_{\text{KL}}(\Pi \parallel P)) \\
&= \sigma_{\varepsilon, \delta}^2 + \frac{T}{T^2} (\lambda_0^2 \text{Var}[r(x_t)] + \mathbb{E}[\log^2 r(x_t)]) \\
&\quad + \frac{1}{T} D_{\text{KL}}(\Pi \parallel P)^2 - \frac{2\lambda_0}{T} (D_{\text{KL}}(P \parallel \Pi) + D_{\text{KL}}(\Pi \parallel P)) \\
&= \sigma_{\varepsilon, \delta}^2 + \frac{1}{T} (\lambda_0^2 \mathbb{E}[r(x_t)^2] - \lambda_0^2 \mathbb{E}^2[r(x_t)] + \mathbb{E}[\log^2 r(x_t)]) \\
&\quad + \frac{1}{T} D_{\text{KL}}(\Pi \parallel P)^2 - \frac{2\lambda_0}{T} (D_{\text{KL}}(P \parallel \Pi) + D_{\text{KL}}(\Pi \parallel P)) \\
&= \sigma_{\varepsilon, \delta}^2 + \frac{1}{T} (\lambda_0^2 \mathbb{E}[r(x_t)^2] - \lambda_0^2 + \mathbb{E}[\log^2 r(x_t)]) \\
&\quad + \frac{1}{T} D_{\text{KL}}(\Pi \parallel P)^2 - \frac{2\lambda_0}{T} (D_{\text{KL}}(P \parallel \Pi) + D_{\text{KL}}(\Pi \parallel P)) \\
&[\because \text{Fact 4.1} \implies \mathbb{E}[r(x_t)] = 1] \\
&= \sigma_{\varepsilon, \delta}^2 + \frac{1}{T} (\lambda_0^2 \mathbb{E}[r(x_t)^2] + \mathbb{E}[\log^2 r(x_t)]) - \frac{\lambda_0^2}{T} \\
&\quad + \frac{1}{T} D_{\text{KL}}(\Pi \parallel P)^2 - \frac{2\lambda_0}{T} (D_{\text{KL}}(P \parallel \Pi) + D_{\text{KL}}(\Pi \parallel P)). \tag{1}
\end{aligned}$$

Recalling that $1 - \frac{1}{x} \leq \log x \leq x - 1 \forall x \in \mathbb{R}_{\geq 0}$, we get

$$\log^2(r(x_t)) \leq \begin{cases} (r(x_t) - 1)^2, & \text{if } r(x_t) \geq 1 \\ (1 - \frac{1}{r(x_t)})^2, & \text{if } r \in (0, 1). \end{cases}$$

Therefore, $\mathbb{E}[\log^2(r(x_t))]$

$$\begin{aligned}
&\leq \max \left\{ \mathbb{E}[(r(x_t) - 1)^2], \mathbb{E} \left[\left(1 - \frac{1}{r(x_t)} \right)^2 \right] \right\} \\
&= \max \left\{ \mathbb{E}[r(x_t)^2] + 1 - 2\mathbb{E}[r(x_t)], 1 + \mathbb{E} \left[\frac{1}{r(x_t)^2} \right] - 2\mathbb{E} \left[\frac{1}{r(x_t)} \right] \right\} \\
&= \max \left\{ \mathbb{E}[r(x_t)^2] - 1, 1 + \mathbb{E} \left[\frac{1}{r(x_t)^2} \right] - 2\mathbb{E} \left[\frac{1}{r(x_t)} \right] \right\} \\
&[\because \text{Fact 4.1} \implies \mathbb{E}[r(x_t)] = 1] \\
&\leq \max \left\{ \mathbb{E}[r(x_t)^2] - 1, 1 + \mathbb{E} \left[\frac{1}{r(x_t)^2} \right] - \frac{2}{\mathbb{E}[r(x_t)]} \right\} \\
&\left[\frac{1}{r(x_t)} \text{ convex } \forall r \in \mathbb{R}^+ \xrightarrow{\text{Jensen's ineq.}} \mathbb{E} \left[\frac{1}{r(x_t)} \right] \geq \frac{1}{\mathbb{E}[r(x_t)]} \right] \\
&= \max \left\{ \mathbb{E}[r(x_t)^2] - 1, \mathbb{E} \left[\frac{1}{r(x_t)^2} \right] - 1 \right\} \\
&\leq \max \left\{ \sum_{x \in \mathcal{X}} \frac{P(x)^2}{\Pi(x)^2} \Pi(x), \sum_{x \in \mathcal{X}} \frac{\Pi(x)^2}{P(x)^2} \Pi(x) \right\} - 1 \\
&= \max \left\{ \sum_{x \in \mathcal{X}} \frac{P(x)^2}{\Pi(x)}, \sum_{x \in \mathcal{X}} \frac{\Pi(x)^3}{P(x)^2} \right\} - 1 \\
&\leq \max \left\{ \sum_{x \in \mathcal{X}} \alpha P(x), \sum_{x \in \mathcal{X}} \beta^2 \Pi(x) \right\} - 1 = \max \{ \alpha, \beta^2 \} - 1. \tag{2}
\end{aligned}$$

Combining (1) and (2) gives us:

$$\begin{aligned}
&\text{Var} \left[D_{\text{KL}}(\Pi \| P)_{\text{est}[\lambda_0, T, \varepsilon, \delta]}^{\text{final}} \right] \\
&\leq \sigma_{\varepsilon, \delta}^2 + \frac{1}{T} (\lambda_0^2 \mathbb{E}[r(x_t)^2] + \max \{ \alpha, \beta^2 \} - 1) - \frac{\lambda_0^2}{T} \\
&\quad + \frac{1}{T} D_{\text{KL}}(\Pi \| P)^2 - \frac{2\lambda_0}{T} (D_{\text{KL}}(P \| \Pi) + D_{\text{KL}}(\Pi \| P)) \\
&= \sigma_{\varepsilon, \delta}^2 + \frac{1}{T} \left(\lambda_0^2 \sum_{x \in \mathcal{X}} \frac{P(x)^2}{\Pi(x)} + \max \{ \alpha, \beta^2 \} - 1 \right) - \frac{\lambda_0^2}{T} \\
&\quad + \frac{1}{T} D_{\text{KL}}(\Pi \| P)^2 - \frac{2\lambda_0}{T} (D_{\text{KL}}(P \| \Pi) + D_{\text{KL}}(\Pi \| P)) \\
&= \sigma_{\varepsilon, \delta}^2 + \frac{1}{T} (\lambda_0^2 \alpha + \max \{ \alpha, \beta^2 \} - 1) - \frac{\lambda_0^2}{T} \\
&\quad + \frac{1}{T} D_{\text{KL}}(\Pi \| P)^2 - \frac{2\lambda_0}{T} (D_{\text{KL}}(P \| \Pi) + D_{\text{KL}}(\Pi \| P)) \\
&= \sigma_{\varepsilon, \delta}^2 + \frac{\lambda_0^2}{T} (\alpha - 1) + \frac{1}{T} (\max \{ \alpha - 1, \beta^2 - 1 \} + D_{\text{KL}}(\Pi \| P)^2) \\
&\quad - \frac{2\lambda_0}{T} (D_{\text{KL}}(P \| \Pi) + D_{\text{KL}}(\Pi \| P)).
\end{aligned}$$

□

A.2 Proof of Theorem 4.10

For $P_1, P_2 \in \mathcal{P}^{>1}$ with $P_1 \sim P_2$, we have $h_1, h_2 \in \mathcal{H}_{\mathcal{X}}^{>1}$ with $h_1 \sim h_2$ satisfying $P_1 = \psi(h_1)$ and $P_2 = \psi(h_2)$. Thus, there are $x_1, x_2 \in \mathcal{X}$ such that $h_1(x_1) - h_2(x_1) = 1$, $h_1(x_2) - h_2(x_2) = -1$ and $h_1(x) = h_2(x) \forall x \in \mathcal{X} \setminus \{x_1, x_2\}$. Let $N = |h_1| = |h_2|$, $n_1 = h_1(x_1)$, and $n_2 = h_1(x_2)$. Note that, as $P_1, P_2 \in \mathcal{P}^{>1}$, $n_1, n_2 \geq 2$. Let $X = x \in \mathcal{X}$ be some realization of $X \sim \Pi$, and, for notational convenience, let $r_i = \frac{P_i(x)}{\Pi(x)}$ and $\lambda_i = \lambda_{0, P_i}$ for $i = 1, 2$ in the context of this proof. We obtain $|\hat{\eta}(P_1) - \hat{\eta}(P_2)|$

$$\begin{aligned}
&= |(\lambda_1(r_1 - 1) - \log r_1) - (\lambda_2(r_2 - 1) - \log r_2)| \\
&= \left| \frac{\lambda_1 P_1(x) - \lambda_2 P_2(x)}{\Pi(x)} + (\lambda_1 - \lambda_2) + \log \frac{P_2(x)}{P_1(x)} \right| \\
&\leq \left| \frac{\lambda_1 P_1(x) - \lambda_2 P_2(x)}{\Pi(x)} \right| + |\lambda_1 - \lambda_2| + \left| \log \frac{P_2(x)}{P_1(x)} \right| \\
&\text{[by triangle-inequality]} \\
&= \left| \frac{\lambda_1 P_1(x) - \lambda_2 P_2(x)}{\Pi(x)} \right| + |\lambda_1 - \lambda_2| + \left| \log \frac{h_2(x)}{h_1(x)} \right| \\
&\left[\because P_i(x) = \frac{h_i(x)}{N} \text{ for } i = 1, 2 \right] \\
&\leq \left| \frac{\lambda_1 P_1(x) - \lambda_2 P_2(x)}{\Pi(x)} \right| + |\lambda_1 - \lambda_2| + \max \left\{ \left| \log \frac{n_1}{n_1 - 1} \right|, \left| \log \frac{n_2 + 1}{n_2} \right| \right\} \\
&\left[\because \forall x \in \mathcal{X} \setminus \{x_1, x_2\}, h_1(x) = h_2(x) \implies \log \frac{h_2(x)}{h_1(x)} = 0 \right] \\
&\leq \max \left\{ \frac{p|\lambda_1 - \lambda_2|}{\Pi(x)}, \frac{|\lambda_1 n_1 - \lambda_2(n_1 - 1)|}{N\Pi(x_1)}, \frac{|\lambda_1 n_2 - \lambda_2(n_2 + 1)|}{N\Pi(x_2)} \right\} \\
&\quad + |\lambda_1 - \lambda_2| + \max \left\{ \log \frac{n_1}{n_1 - 1}, \log \frac{n_2 + 1}{n_2} \right\} \\
&\text{[where } p = h_1(x)/N = h_2(x)/N \forall x \in \mathcal{X} \setminus \{x_1, x_2\}] \\
&\leq \max \left\{ \hat{\alpha}|\lambda_1 - \lambda_2|, \frac{|n_1(\lambda_1 - \lambda_2) + \lambda_2|}{N\Pi(x_1)}, \frac{|n_2(\lambda_1 - \lambda_2) - \lambda_2|}{N\Pi(x_2)} \right\} \\
&\quad + |\lambda_1 - \lambda_2| + \max \left\{ \log \frac{n_1}{n_1 - 1}, \log \frac{n_2 + 1}{n_2} \right\} \\
&\leq \max \left\{ \hat{\alpha}|\lambda_1 - \lambda_2|, \frac{|n_1(\lambda_1 - \lambda_2)| + |\lambda_2|}{N\Pi(x_1)}, \frac{|n_2(\lambda_1 - \lambda_2)| + |\lambda_2|}{N\Pi(x_2)} \right\} \\
&\quad + |\lambda_1 - \lambda_2| + \max \left\{ \log \frac{n_1}{n_1 - 1}, \log \frac{n_2 + 1}{n_2} \right\} \\
&\leq \max \left\{ \hat{\alpha}|\lambda_1 - \lambda_2|, \hat{\alpha}|\lambda_1 - \lambda_2| + \frac{\lambda_2}{N\Pi(x_1)}, \hat{\alpha}|\lambda_1 - \lambda_2| + \frac{\lambda_2}{N\Pi(x_2)} \right\} \\
&\quad + |\lambda_1 - \lambda_2| + \max \left\{ \log \frac{n_1}{n_1 - 1}, \log \frac{n_2 + 1}{n_2} \right\} \\
&= (\hat{\alpha} + 1)|\lambda_1 - \lambda_2| + \frac{\lambda_2}{N} \max \left\{ \frac{1}{\Pi(x_1)}, \frac{1}{\Pi(x_2)} \right\} + \max \left\{ \log \frac{n_1}{n_1 - 1}, \log \frac{n_2 + 1}{n_2} \right\}
\end{aligned}$$

$$\begin{aligned}
&\leq (\hat{\alpha} + 1)|\lambda_1 - \lambda_2| + \frac{\lambda_2}{Nm} + \max \left\{ \log \frac{n_1}{n_1 - 1}, \log \frac{n_2 + 1}{n_2} \right\} \\
&\leq (\hat{\alpha} + 1)|\lambda_1 - \lambda_2| + \frac{\lambda_2}{Nm} + \max \left\{ \log \left(1 + \frac{1}{n_1 - 1} \right), \log \left(1 + \frac{1}{n_2} \right) \right\} \\
&\leq (\hat{\alpha} + 1)|\lambda_1 - \lambda_2| + \frac{\lambda_2}{Nm} + \max \left\{ \log \left(1 + \frac{1}{2 - 1} \right), \log \left(1 + \frac{1}{2} \right) \right\} \\
&= (\hat{\alpha} + 1)|\lambda_1 - \lambda_2| + \frac{\lambda_2}{Nm} + \log 2.
\end{aligned}$$

□

References

- [1] J. F. McCarthy, K. A. Marx, P. E. Hoffman, A. G. Gee, P. O’Neil, M. L. Ujwal, and J. Hotchkiss. Applications of machine learning and high-dimensional visualization in cancer detection, diagnosis, and management. In *Annals of the New York Academy of Sciences*, 1020(1):239-262. Wiley Online Library, 2004.
- [2] M. M. Najafabadi, F. Villanustre, T. M. Khoshgoftaar, N. Seliya, R. Wald, and E. Muharemagic. Deep learning applications and challenges in big data analytics. In *Journal of Big Data*, 2:1-21. Springer, 2015.
- [3] A. Bharadwaj and G. Cormode. An introduction to federated computation. In *Proceedings of the 2022 International Conference on Management of Data*, pages 2448-2451. ACM, 2022.
- [4] P. Kairouz, H. B. McMahan, B. Avent, A. Ballet, M. Bennis, A. N. Bhagoji, K. A. Bonawitz, Z. Charles, G. Cormode, R. Cummings, R. G. L. D’Oliveira, H. Eichner, S. El Rouayheb, D. Evans, J. Gardner, Z. Garrett, A. Gascón, B. Ghazi, P. B. Gibbons, M. Gruteser, Z. Harchaoui, C. He, L. He, Z. Hou, B. Hutchinson, J. Hsu, M. Jaggi, T. Javidi, G. Joshi, M. Khodak, J. Konečný, A. Korolova, F. Koushanfar, S. Koyejo, T. Lepoint, Y. Liu, P. Mittal, M. Mohri, R. Nock, A. Özgü, R. Pagh, H. Qi, D. Ramage, R. Raskar, M. Raykova, D. Song, W. Song, S. U. Stich, Z. Sung, A. T. Suresh, F. Tramèr, P. Vepakomma, J. Wang, Li, Xiong, Z. Xu, Q. Yang, F. X. Yu, H. Yu, and S. Zhao. Advances and open problems in federated learning. In *Foundations and Trends in Machine Learning*, 14(1-2):1-210, 2021.
- [5] M. Abadi, A. Chu, I. J. Goodfellow, H. B. McMahan, I. Mironov, K. Talwar, and L. Zhang. Deep learning with differential privacy. In *Proceedings of the 2016 ACM SIGSAC Conference on Computer and Communications Security, Vienna, Austria, October 24-28, 2016*, pages 308-318. ACM, 2016.
- [6] K. Bonawitz, V. Ivanov, B. Kreuter, A. Marcedone, B. McMahan, S. Patel, D. Ramage, A. Segal, and K. Seth. Practical secure aggregation for privacy-preserving machine learning. In *Proceedings of the 2017 ACM SIGSAC Conference on Computer and Communications Security*, pages 1175-1191, 2017.

- [7] S. Kullback and R. A. Leibler. On information and sufficiency. In *The Annals of Mathematical Statistics*, 22(1):79-86. Institute of Mathematical Statistics, 1951.
- [8] C. Dwork and A. Roth. The algorithmic foundations of differential privacy. *Foundations and Trends in Theoretical Computer Science*, 9(3-4):211-407, 2014.
- [9] B. McMahan, E. Moore, D. Ramage, S. Hampson, and B. A. y Arcas. Communication-efficient learning of deep networks from decentralized data. In *International Conference on Artificial Intelligence and Statistics*, pages 1273-1282. PMLR, 2017.
- [10] S. Guha, P. Indyk, and A. McGregor. Sketching information divergences. In *20th Annual Conference on Learning Theory*, pages 424-438. Springer, 2007.
- [11] J. Blocki, A. Blum, A. Datta, and O. Sheffet. The Johnson-Lindenstrauss Transform itself preserves differential privacy. In *2012 IEEE 53rd Annual Symposium on Foundations of Computer Science*, pages 410-419. IEEE Computer Society, 2012.
- [12] K. Kenthapadi, A. Korolova, I. Mironov, and N. Mishra. Privacy via the Johnson-Lindenstrauss Transform. In *Journal of Privacy and Confidentiality*, 5(1):39-71, 2013.
- [13] C. Hou, H. Zhan, A. Shrivastava, S. Wang, A. Livshits, G. Fanti, and D. Lazar. Privately customizing prefinetuning to better match user data in federated learning. *arXiv preprint arXiv:2302.09042*, 2023.
- [14] F. Nielsen, K. Sun, and S. Marchand-Maillet. On Hölder projective divergences. In *Entropy*, 19(3):122. MDPI, 2017.
- [15] A. Andoni, K. Do Ba, P. Indyk, and D. Woodruff. Efficient sketches for earth-mover distance, with applications. In *2009 50th Annual IEEE Symposium on Foundations of Computer Science*, pages 324-330. IEEE, 2009.
- [16] M. Heikkilä, J. Jälkö, O. Dikmen, and A. Honkela. Differentially private Markov chain Monte Carlo. In *Advances in Neural Information Processing Systems*, 32:1-11, 2019.
- [17] J. R. Hershey and P. A. Olsen. Approximating the Kullback Leibler divergence between Gaussian mixture models. In *2007 IEEE International Conference on Acoustics, Speech and Signal Processing-ICASSP'07*, 4:IV-317. IEEE, 2007.
- [18] M. Heikkilä, E. Lagerspetz, S. Kaski, K. Shimizu, S. Tarkoma, and A. Honkela. Differentially private Bayesian learning on distributed data. In *Advances in Neural Information Processing Systems*, 30:1-10, 2017.

- [19] H. Corrigan-Gibbs and D. Boneh. Prio: Private, robust, and scalable computation of aggregate statistics. In *14th USENIX Symposium on Networked Systems Design and Implementation (NSDI 17)*, pages 259-282. USENIX, 2017.
- [20] S. Addanki, K. Garbe, E. Jaffe, R. Ostrovsky, and A. Polychroniadou. Prio+: Privacy preserving aggregate statistics via boolean shares. In *International Conference on Security and Cryptography for Networks*, pages 516-539. Springer, 2022.
- [21] D. Keeler, C. Komlo, E. Lepert, S. Veitch, and X. He. DPrio: Efficient differential privacy with high utility for Prio. In *Proceedings on Privacy Enhancing Technologies*, 2023(3):375-390, 2023.
- [22] J. Kim, G. Park, M. Kim, and S. Park. Cluster-based secure aggregation for federated learning. In *Electronics*, 12(4):870. MDPI, 2023.
- [23] A. Shamir. How to share a secret. In *Communications of the ACM*, 22(11):612-613. ACM, 1979.
- [24] A. Shapiro. Monte Carlo sampling methods. In *Handbooks in Operations Research and Management Science*, 10:353-425. Elsevier, 2003.
- [25] S. Amari. α -Divergence Is Unique, Belonging to Both f -Divergence and Bregman Divergence Classes. In *IEEE Transactions on Information Theory*, 55(11):4925-4931. IEEE, 2009.
- [26] S. S. Dragomir and V. Glušćević. Some inequalities for the Kullback-Leibler and χ^2 -distances in information theory and applications. In *RGMA Research Report Collection*, 3(2):199-210. School of Communications and Informatics, Faculty of Engineering and Science, 2000.
- [27] S. Caldas, S. M. K. Duddu, P. Wu, T. Li, J. Konečný, H. B. McMahan, V. Smith, and A. Talwalkar. LEAF: A benchmark for federated settings. *arXiv preprint arXiv:1812.01097*, 2018.
- [28] B. Ding, J. Kulkarni, and S. Yekhanin. Collecting telemetry data privately. In *Advances in Neural Information Processing Systems*, pages 3571-3580, 2017.
- [29] M. Scott, G. Cormode, and C. Maple. Aggregation and transformation of vector-valued messages in the shuffle model of differential privacy. In *IEEE Transactions on Information Forensics and Security*, 17:612-627. IEEE, 2022.
- [30] Y. Xiao and L. Xiong. Protecting locations with differential privacy under temporal correlations. In *Proceedings of the 22nd ACM SIGSAC Conference on Computer and Communications Security*, pages 1298-1309. ACM, 2015.
- [31] Z. Jorgensen, T. Yu, and G. Cormode. Conservative or liberal? Personalized differential privacy. In *2015 IEEE 31st International Conference on Data Engineering*, pages 1023-1034. IEEE, 2015.

- [32] K. Bonawitz, F. Salehi, J. Jakub Konečný, B. McMahan, and M. Gruteser. Federated learning with autotuned communication-efficient secure aggregation. In *2019 53rd Asilomar Conference on Signals, Systems, and Computers*, pages 1222-1226. IEEE, 2019.
- [33] P. Kairouz, K. Bonawitz, and D. Ramage. Discrete distribution estimation under local privacy. *International Conference on Machine Learning*, 48:2436-2444. PMLR, 2016.
- [34] P. Kairouz, Z. Liu, and T. Steinke. The distributed discrete gaussian mechanism for federated learning with secure aggregation. In *International Conference on Machine Learning*, pages 5201-5212. PMLR, 2021.